scientific reports

Check for updates

OPEN

Environmental benign catalyst developed by fruit waste for synthesis of β-amino alcohol with the optimum combination through statistical analysis

Richa Tiwari[1], Prashant Bhati[1], Narendra Pal Lamba[1], Jagdish Prasad[1], Vijay Bahadur[3], Umesh Kumar Sharma[4], Sonia Chahar Srivastava[2]✉ & Manmohan Singh Chauhan[1]✉

An Eco-catalysis approach reported in this manuscript, is developed by the kinnow peel waste as the green catalyst for the ring opening of epichlorohydrin with aromatic amines and its derivatives. The prepared green catalyst is used in three different variants i.e. kinnow peel powder (KPP), Bare component, and ash of KPP. Prepared catalyst characterized by TEM, SEM-EDX, FTIR, TGA, and XRD. Statistical analysis is a full factorial analysis of variance technique to identify the optimum combinations of types of catalyst, catalyst quantity, and derivative type.

Keywords Eco-catalyst, Green catalyst, Ring-opening, β-amino alcohol, Statistical analysis

In synthetic organic chemistry and medicinal chemistry, epoxides are very important because they provide multiple functional groups containing building blocks[1,2]. The nucleophilic ring opening of epoxide with amines is an important route to provide various functional groups containing chemical scaffolds, including β-amino alcohols[3].

Many bioactive compounds, chiral auxiliaries, unnatural amino acids, and organocatalysts are prepared by β-Amino alcohols as intermediate[4–9]. In pharmaceutical industries, β-amino alcohols are used as heart medications (I), anti-asthma medications (II), antimalarial medications (III), hypertension medications (IV), -blockers, antibacterial and hypoglycemic medications, etc[10–13], anti-fungal medications[14] HIV protease inhibitors[15] and anti-Alzheimer agents[16,17], etc. A flexible synthesis strategy is required for the preparation of β-amino alcohols due to their high importance in chemical synthesis and pharmaceutical research. Ring-opening reactions of epoxide have been reported with various types of catalysts including Bismuth (III) salts[18–21], Lewis's acids[22–24], and metal-organic frameworks[25]. Additionally, polymerization reactions of epoxide[26] and 3-glycidyloxypropyltrimethoxysilane (GPTS)[27,28] were also performed by different catalysts.

These techniques, which have unfavorable side effects and necessitate costly reagents and high catalyst loadings that offer poor regioselectivity, were described for epoxide rearrangement to allyl alcohols under extremely alkaline conditions or polymerization under strongly acidic conditions. These methods also require toxic and hazardous reagents which are harmful to ecology and environment. Furthermore, the processing of these chemicals is a major difficulty to remove the complications and recycling of these chemicals. To address these problems, a straightforward, dynamic, and environmentally friendly synthetic approach must be developed.

Recently, many protocols have been developed for the ring-opening reaction of epoxides to produce amino alcohols using green and easy methods. It is an important protocol in organic synthesis to construct vicinal bifunctional groups by ring opening of epoxide with nucleophiles. Ultrasonic synthesis[29], in situ spectroscopic techniques[30,31], and microwave[32–34] have been reported as green chemical methods and some topics in these areas are directly relevant to green chemistry.

The primary objective of green chemistry is to decrease the usage of reagents and chemical processes that result in the generation of hazardous or dangerous compounds[35]. In addition, the newly coined "Eco-catalysis"

[1]Amity University Rajasthan, Jaipur 303002, India. [2]Department of Chemistry, SS Jain Subodh PG (Autonomous) College, Jaipur 302005, India. [3]Department of Science, Alliance University, Bengaluru 562106, Karnataka, India. [4]Department of Polymer Science, Bhaskaracharya College of Applied Sciences, University of Delhi, Delhi 110075, India. ✉email: soniachahar@gmail.com; phd8du@gmail.com

term provides the synthetic route for organic molecules which is based on sustainable and greener processes. Grison introduced a new concept in catalysis termed "Eco-catalysis"[36–38]. The biobased approach of Eco-catalysts provides many benefits of homogeneous and heterogeneous catalysts, such as selectivity, activity, and recyclability. By focusing on the ecological restoration of contaminated ecosystems, Eco-catalysis is laying the groundwork for the catalytic chemistry tools of the future.

Biomass is a cheap carbon material, so, it is important and abundant in nature[39]. Biomass has great potential because of its chemical, mechanical, and physical properties and it is derived from mesoporous carbon[40,41]. Hence, biomass has a wide range of applications including in the field of sensors[42–44], catalysis[45–49], gas storage[50–52], energy storage[53–58], and waste-water treatment[59,60]. Recently Verma et al. reported the kinnow peel powder for Schiff base reaction.[61]

Biomass is a suitable catalytic support material because it has many oxygen functional groups and other components at its surface. Many biomass-based catalysts have been reported which are obtained from fruit peels but they were found inefficient for catalytic purposes[62–64], for example as a fruit pulp-based catalyst created from waste *Citrus limetta* (Mausambi)[65,66]. Therefore, it is essential to create new biomass-based catalysts that are more dependable and stable for a variety of applications.

Due to the significant value of environmentally friendly catalysis and the potential for cost-effectiveness, the present study based on waste fruit peel, has been reported to examine its possible use as a catalyst for ring opening of epoxide.

Herein, it is reported that the catalysis process of environmentally friendly and sustainable chemistry is based on the well-known idea of eco-catalysis[37,38,67,68]. Eco-catalysis sits at the nexus of sustainable chemistry and scientific ecology. The reported catalytic route not require high temperature and pressure which provides an alternate sustainable approach for low or negligible energy catalytic system[69].

Materials and methods

Materials

In this study, waste peels from *Kinnow mandarin* are chosen and employed as an Eco catalyst. Waste kinnow Peel is collected from a neighborhood fruit market in Dausa, Rajasthan. Transmission emission spectroscopy (TEM), X-ray diffraction (XRD), thermogravimetric analysis (TGA), energy dispersion Xray spectroscopy (EDS), Fourier transform infrared spectroscopy (FT-IR), scanning electron microscopy (SEM), and thin layer chromatography (TLC) are some of the methods used to characterize kinnow peel powder. All chemicals and solvents DCM, acetonitrile, hexane, toluene, CCl_4, acetonitrile, aniline, and its derivatives, epichlorohydrin are used without any purification.

Preparation of the catalyst

Waste Kinnow peel are cleaned thoroughly and then rinsed with deionized water to remove any remaining dirt. Next, the kinnow peel was cut into pieces. The peel is dried for 24 h at 60 °C in an oven to eliminate moisture content. Alternatively, kinnow peel can be dried in sunlight to keep for 3–5 days. After completing the drying process, the dried peel is converted into a powder by using the grinder for 15 min and sieved to obtain particles of < 155 µm size, which are then kept for use in further catalytic experiments. (Fig. 1). Such collected material is kept in a vacuum desiccator and directly used as a catalyst without any chemical modification. It does not require any specific reaction condition to prepare the catalytic system as reported in previous literature[70]. Prepared catalyst follows the greener route and sustainable methods. The reported method also not use any combustion method to avoid NOx emission.[71]

The catalytic reaction of Kinnow Peel powder in the ring opening of epoxide with amine

30 mg of kinnow peel powder (KPP) was taken in a 50 ml round bottom flask and given it high vacuum to activate the KPP by removing moisture content. After that, 1 mmol of epichlorohydrin was added to it and allowed to stir at room temperature for 10 min. After 10 min, 1 mmol of aniline was added to it and allowed to stir at room temperature for 24 h. The progress of the reaction was checked by TLC. After completion of the reaction, the desired product was obtained by column chromatography with hexane and ethyl acetate in an 8:2 ratio to purify the catalytic product. A similar procedure is applied to the reaction between epichlorohydrin and amine derivatives.

Results and discussion

The optimization of the catalytic reaction is performed with different solvents, and different catalyst loading to obtain the best yield of catalytic products (Fig. 2).

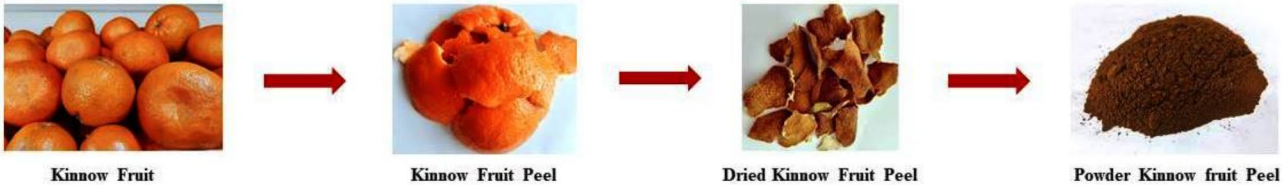

Fig. 1. Schematic representation of preparation of the catalyst.

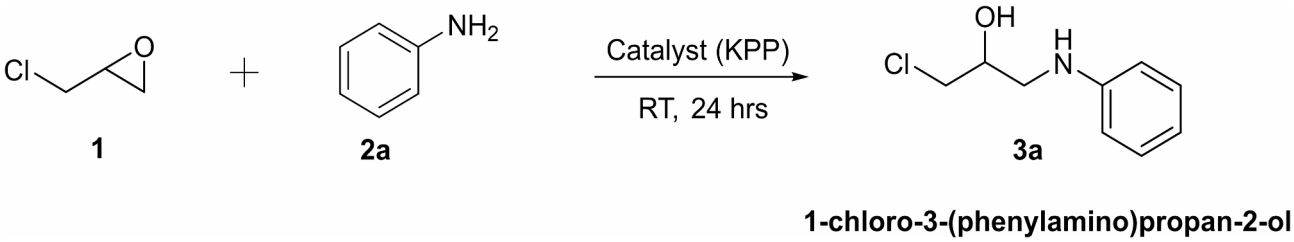

Fig. 2. Ring opening of epichlorohydrin with aniline.

Entry	Solvents	Catalyst (mg)	Time (h)	Yield (%)
1	DCM	10	24	24
2	Toluene	10	24	35
3	CCl_4	10	24	22
4	Hexane	10	24	20
5	Acetonitrile	10	24	38
6	THF	10	24	26
7	Neat	10	24	32
8	Neat	20	24	40
9	Neat	30	24	53
10	Neat	Without catalyst	24	No reaction
11	Neat	Bare component	24	20
12	Neat	Carbonized	24	No reaction

Table 1. The impact of various catalyst concentrations and solvents on the ring opening of epichlorohydrin with aniline.

Entry	Amine (*R*)	Yield (%)
1	4-NO_2	32
2	4-OCH_3	58
3	4-Br	35

Table 2. Reaction of different derivatives of amines with epichlorohydrin.

The ring-opening reaction of epichlorohydrin with aniline was carried out with different solvents and the observed yield of β-amino alcohol is mentioned in Table 1. DCM yields a relative product of 24% (Table 1, entry 1), but toluene yields only 35% (Table 1, entry 2). Additionally, we opened the ring of epichlorohydrin with amine using CCl_4, hexane, acetonitrile, and THF; 22–26% of the related products were obtained, accordingly (Table 1, entries 3–6). Additionally, we looked into the impact of catalyst loading and found that 10 mg of the catalyst produced reasonable results (Table 1, entry 7), while 30 mg of the catalyst produced the highest yield of β-amino alcohol but no product was formed in the absence of catalyst (Table 1, entry 10). A low yield (20%) of relative product is likewise provided by the bare component (Table 1, entry 11).

As a result, Kinnow peel powder (KPP) is an extremely reliable and environmentally acceptable catalyst for β-amino alcohol synthesis, giving the best results in mild reaction conditions.

We have also used different derivatives of aniline like 4-nitro, 4-methoxy, and 4-bromo with epichlorohydrin to synthesize the β-amino alcohol using optimized reaction conditions i.e.30 mg of KPP used as catalyst at room temperature for 24 h. The observed results are shown in Table 2 and it is found that 4-methoxy aniline provides a better yield i.e. 58% of relative β-amino alcohol (Table 2, entry 2) than 4-nitro and 4-bromo aniline which provides 32% and 35% yield of relative β-amino alcohol (Table 2, entry 1 & 3) (Fig. 3).

Statistical analysis of catalytic reaction to find out optimum combination

Three factors are involved in the catalytic reaction i.e. type of catalyst (tcl), catalyst loading (cl), and derivative type. In this study, three types of catalyst kinnow peel powder (KPP), ash of KPP: and bare part; three types of catalyst loading 10 mg, 20 mg, 30 mg and four types of amines derivates i.e. Aniline, 4-nitroaniline, 4-methoxy aniline, 4-bromoaniline. So there are three factors, the first factor, the second factor has three levels and the third factor has four levels. Therefore, it is a (3*3*4) factorial experiment with 36 treatment combinations. These 36 treatment combinations are replicated three times. So, the total number of observations is taken 108. Taking a

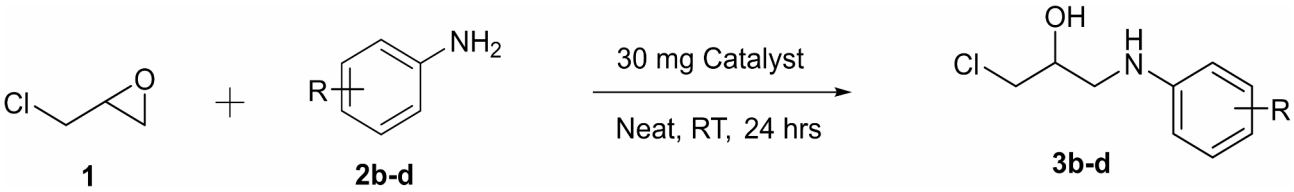

Fig. 3. Ring opening of epichlorohydrin with amine.

Tests of between-subjects effects					
Dependent variable: Yield					
Source	**Type III sum of squares**	**df**	**Mean square**	**F**	**Sig.**
Corrected model	17652.250[a]	35	504.350	648.450	0.000
Intercept	287370.750	1	287370.750	369476.679	0.000
Amine	6544.694	3	2181.565	2804.869	0.000
CL	1987.722	2	993.861	1277.821	0.000
TCL	5454.056	2	2727.028	3506.179	0.000
Amine × CL	681.611	6	113.602	146.060	0.000
Amine × TCL	900.833	6	150.139	193.036	0.000
CL × TCL	637.556	4	159.389	204.929	0.000
Amine × CL × TCL	1445.778	12	120.481	154.905	0.000
Error	56.000	72	0.778		
Total	305079.000	108			
Corrected total	17708.250	107			

Table 3. Tests of between-subjects effects. [a]R Squared = 0.997 (Adjusted R Squared = 0.995).

single observation of the yield of each treatment combination does not provide a reliable inference. From these 108 observations, the following objectives will be archived through the analysis of variance (ANOVA) technique.

Objectives:

(1) To examine the distinct impacts on reaction yield of several catalyst types catalyst loading and amine's derivative.
(2) To examine the effects of pairwise interactions between catalyst type, catalyst loading, and amine's derivative.
(3) To examine the effect of interaction among the three factors—catalyst type, catalyst loading, and amine's derivative.
(4) To determine the optimum combinations of these three factors' interaction.

To archive the above objectives data were uploaded on SPSS version 26 and statistical analysis was done.

Levene's test of equality of variances was applied to the data and obtained the nul hypothesis that the error variance of the dependent variable (yield) is equal across groups and developed a statistical model.

$$\text{Yield} = \text{intercept} + \text{CL} + \text{TCL} + \text{Amine} + \text{Amine} * \text{CL} + \text{Amine} * \text{TCL} + \text{CL} * \text{TCL} + \text{Amine} * \text{Cl} * \text{TCL}$$

The Table 3 shows that all the main effects, 2-factor interactions, and 3 factor interactions show a significant difference. The above model gives the adjusted $R^2 = 0.995$ i.e. factors and their interactions contribute to an increase in the yield is 99.5% which is very high. This shows the validation of the model used in the analysis of variance.

The above table shows that there is a significant difference among different types of catalyst, catalyst loading, and amine derivatives with regards to yield. The pairwise interactions among the types of derivatives, catalyst loading, and amines derivatives are also significant because the p values given in the last column of the table which is less than 0.05. The three factors' interaction among the types of derivatives, catalyst loading, and amines derivative is also significant. Since the above analyses have significant differences therefore the Post Hoc Test is applied.

Post hoc tests

As shown in Table 3, there is a significant difference among the various levels of types of catalyst, catalyst loading, amines derivatives. From the post hoc test, it is observed that a catalyst loading of 30 mg produces the highest reaction yield with a significant difference observed 10 mg and 20 mg of catalyst loading. Similarly, it is observed that the level of amines derivatives 4-methoxy aniline provides the highest reaction yield and has a significant difference with 4-nitroaniline, 4-bromoaniline, and aniline. Similarly, if we compare the three levels of types of catalyst kinnow peel shows the highest reaction yield and it also shows a significant difference with a level of bare and ash.

Likewise, the Post hoc test (Table 4) is also used to examine different combinations of levels of two-factor interactions. It is observed that the maximum reaction yield was achieved when the type of derivative was 4-methoxy aniline and the catalyst loading was 30 mg. This combination of levels of two-factor interactions was found to differ significantly from the other eleven combinations. Therefore, the highest reaction yield is achieved with a catalyst loading of 30 mg and an amine derivative of 4-methoxy aniline.

Subsequently, it is also observed that the two-factor levels of the type of derivative and catalyst maximized the reaction yield when the type of catalyst was K-peel and the type of derivative was 4-methoxy aniline. These combinations also demonstrated a noteworthy distinction from the other eleven combinations of the levels of the two-factor interactions. The two levels of the interaction between the type of catalyst and catalyst loading. It is observed that the maximum reaction yield was obtained when the type of catalyst was K-peel and the catalyst loading was 30 mg. These combinations also demonstrated a significant difference from the other eight combinations of the levels of the two-factor interactions. It was observed that the maximum reaction yield was obtained when we used K-peel as the type of catalyst and 30 mg as the catalyst loading in the pairwise interaction of catalyst type and catalyst loading. Similarly, the post hoc test was applied to compare the different levels of different factors. The best combinations of three factors the type of catalyst, catalyst loading, and amine derivatives give the maximum reaction yield when the type of catalyst is K-peel, the amount of catalyst is 30 mg, and the type of derivative is 4-methoxy aniline, respectively. This combination shows a significant difference from the other 35 combinations. The optimization result of K-peel, the amount of catalys 30, and the type of derivative is 4-methoxy aniline provide the confidence interval of a lower limit of 78.318 and upper limit of 80.348.

The IR spectrum of fresh Kinnow Peel powder[72]

The IR spectra of KPP shown in Fig. 4, which demonstrate the presence of hydroxyl groups in KPP by the presence of a notable peak at 3328 cm^{-1} in the high-frequency region related to the -OH bond's stretching mode. At 2915 cm^{-1}, the -CH atom is observed to be stretched. The peak at 1609 cm^{-1} is caused by the -C = C aromatic rings. The peak at 1018 cm^{-1}, however, represents the vibrational mode of the -C-O group. IR study confirms the presence of various functional groups in kinnow peel powder. Furthermore, the IR spectra of recovered kinnow peel powder (KPP) were also observed and shown in Fig. 5, which is similar to Fig. 4 and demonstrates the peaks for the presence of -OH bond, -C = C, and -C-O- group.

TEM (Transmission Electron Microscopy)

The morphology of kinnow peel powder is studied using TEM. According to TEM scans, the particles are mostly agglomerate at 200 nm and are spherical with a diameter of > 100 nm and rod-shaped with a length of > 50 nm (Fig. 6). The larger and more varied sizes of KPP's particles are visible in the TEM images. The size of the particle also affects the ring opening of epichlorohydrin. The surface chemistry and structure of a catalyst particle, which ultimately affects catalytic performance, are closely connected to these size and shape-dependent factors.[73] This is because of surface adsorption, which is an essential elemental step, causes a catalytic event on a catalytic site of the catalyst surface at a solid–gas or solid-liquid interface.

SEM-EDX analysis

The morphology of the Kinnow peel powder particles was investigated using SEM. Figure 7 displays the particle core spectra that were acquired in the SEM using EDX. Various morphologies of irregular particles are seen by the SEM spectra. Image J yielded a diameter measurement of 0.95 m for the particle. Shape and surface structure can affect the catalytic reactivity and selectivity.[73] Similar particle sizes and shapes were observed in SEM images of the recovered KPP catalyst which is shown in Fig. 8. Figure 9 displays the results of the EDX analysis for the KPP particle's fractured surface following autoclaving. The catalyst is made up of three elements in total: carbon (C), calcium (Ca), and oxygen (O), which together account for its major (93.9%) and minor (6.1%) components.

TukeyHSD Type of derivative of Amine	(I)Amine	(J)Amine	Mean difference (I – J)	Std. error	Sig.	95% confidence interval	
						Lower bound	Upper bound
	2.00	0.00	18.3333*	0.24003	0.000	17.7020	18.9646
		1.00	14.0000*	0.24003	0.000	13.3687	14.6313
		3.00	1.9259*	0.24003	0.000	1.2946	2.5572
Tukey HSD Catalyst loading cl	**(I)cl**	**(J)cl**	**Mean difference (I – J)**	**Std. error**	**Sig.**	**95% confidence interval Lower bound**	**95% confidence interval Upper bound**
	2.00	0.00	9.6389*	0.20787	0.000	9.1414	10.1363
		1.00	1.1944*	0.20787	0.000	0.6970	1.6919
Tukey HSD Type of catalyst loadind(TCL)	**(I)TCL**	**(J)TCL**	**Mean difference (I – J)**	**Std. error**	**Sig.**	**95% confidence interval Lower bound**	**95% confidence interval Upper bound**
	0.00	1.00	17.3056*	0.20787	0.000	16.8081	17.8030
		2.00	10.2778*	0.20787	0.000	9.7803	10.7752

Table 4. Multiple comparison dependent variable yield.

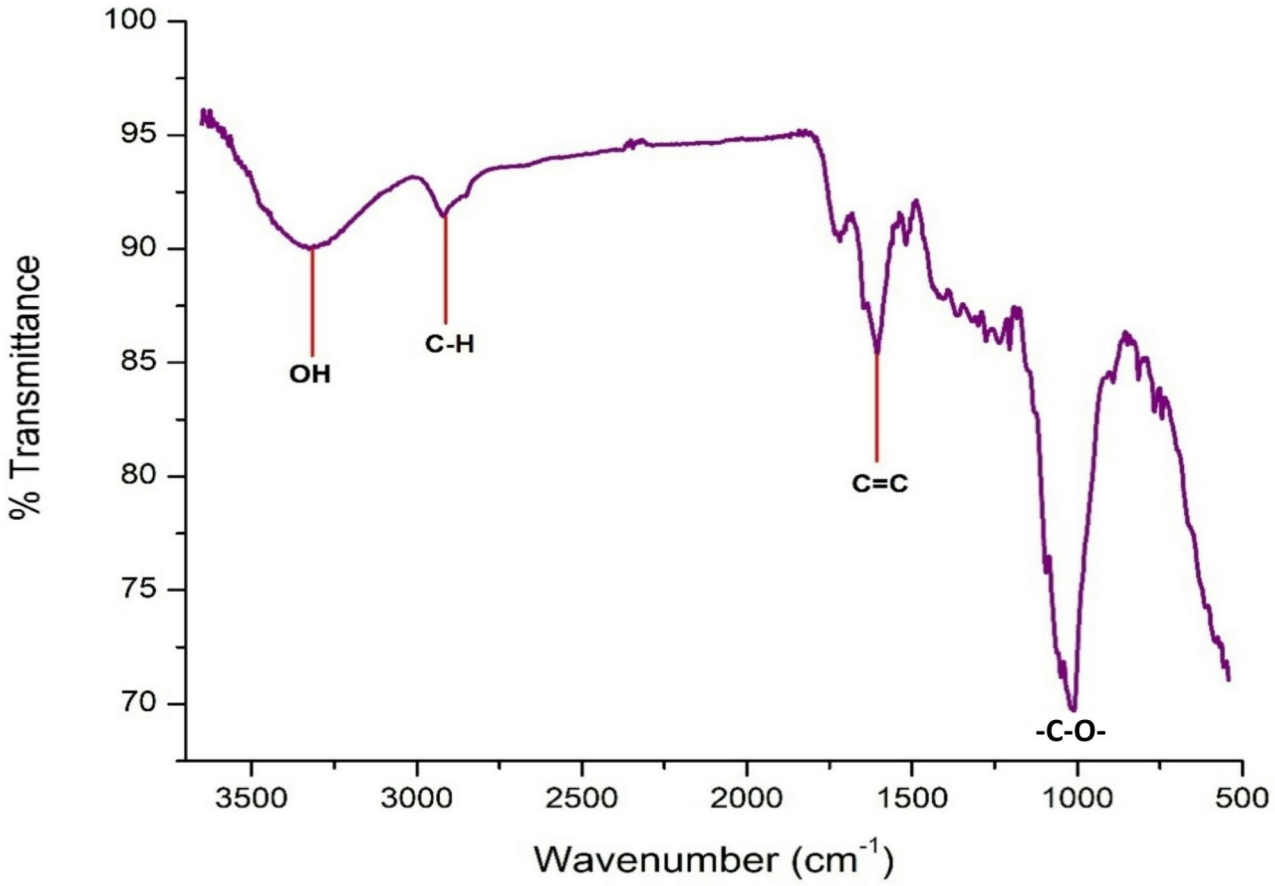

Fig. 4. IR spectrum of Kinnow peel powder (KPP).

TGA analysis

Through a temperature range of 25 °C to 800 °C, the thermogravimetric analysis (TGA) verified the thermal stability of kinnow peel powder. The weight loss below 200 °C was most likely caused by the solvents being chemisorbed and physisorbed off the surface of the Kinnow peel powder. The organic content of KPP getting significant weight loss from a temperature range of 250 °C up to 500 °C (Fig. 10). The initial weight loss of KPP due to the moisture and bonding water evaporation observed in the region of 25 –210 °C. The dehydrated biomass begins to decompose in the temperature range of 210 –520 °C and is attributed to the degradation of hemicellulose, cellulose, and lignin.[72]

XRD pattern of the catalyst

Figure 11 depicts the XRD of kinnow peel powder. Structure, phase, and other information are all available by XRD. The powder quality of the component can be identified by three peaks at 2 values of 15.4, 19.5, and 21 (Figure 11) which corresponds to the crystalline structure of cellulose.

GC-MS analysis of catalytic product

The catalytic products have been characterized by the GC-MS study. After completion of the catalytic reaction, a crude reaction mixture is used for GC-MS study. GC MS of 1-chloro-2-(phenylamino)ethan-1-ol in shown in Fig. 12 (a) which is similar of previously reported literature.[74] As shown in Fig. 12(a), m/z = 185 denoted for parental ion peak, m/z = 106.1 represented for $[C_7H_8N]^{\bullet}$ while m/z = 77.1 is observed for $[C_6H_5]^{+}$. Figure 12 (b) represents the GC-MS spectra for 1-chloro-3-((4-nitrophenyl)amino)propan-2-ol in which molecular ion peak observed at m/z = 230.1 while m/z = 228.1 is observed for $[C_9H_9ClN_2O_3]^{\bullet}$. Unreacted amine and epichlorohydrin is observed at m/s = 136 and m/z 92.1 respectively.

GC-MS spectra of 1-chloro-3-((4-methoxyphenyl)amino)propan-2-ol is shown in Fig. 12 (c) which is similar to previously reported literature[75]. Molecular ion peak observed at m/z = 214 [M-1] while a highly intense peak was observed at m/z = 150.2 for $[C_8H_8NO_2]^{\bullet}$.

Figure 12 (d) shows the GC-MS spectra of 1-((4-bromophenyl)amino)-3-chloropropan-2-ol in which molecular ion peak was observed at m/z = 264 with less intensity. The characteristic isotope peak of bromine (Br^{79} and Br^{81}) is observed at m/z = 253 and 251. A highly intense peak observed at m/z = 92.1 is dedicated for unreacted epichlorohydrin.

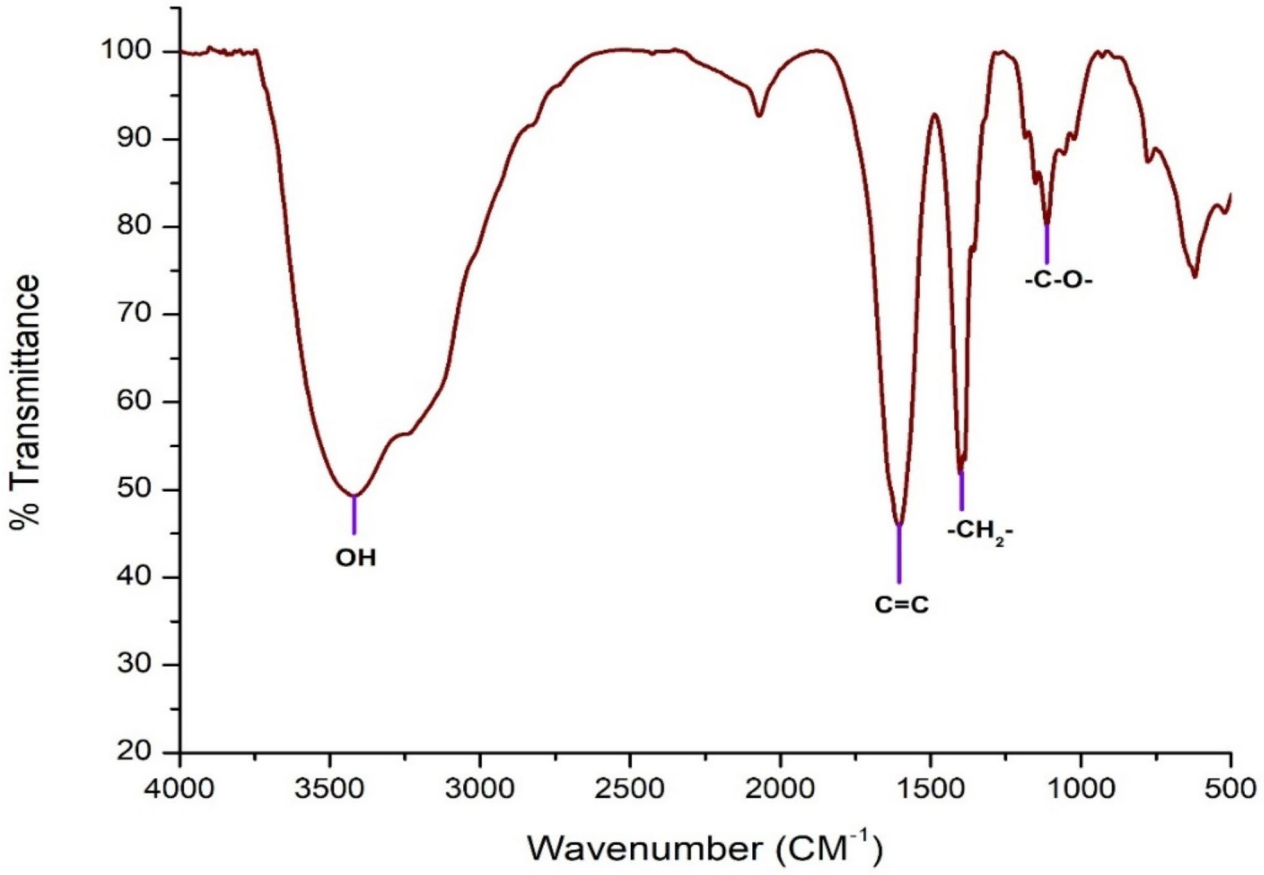

Fig. 5. IR spectrum of recovered Kinnow peel powder (KPP) after catalytic reaction.

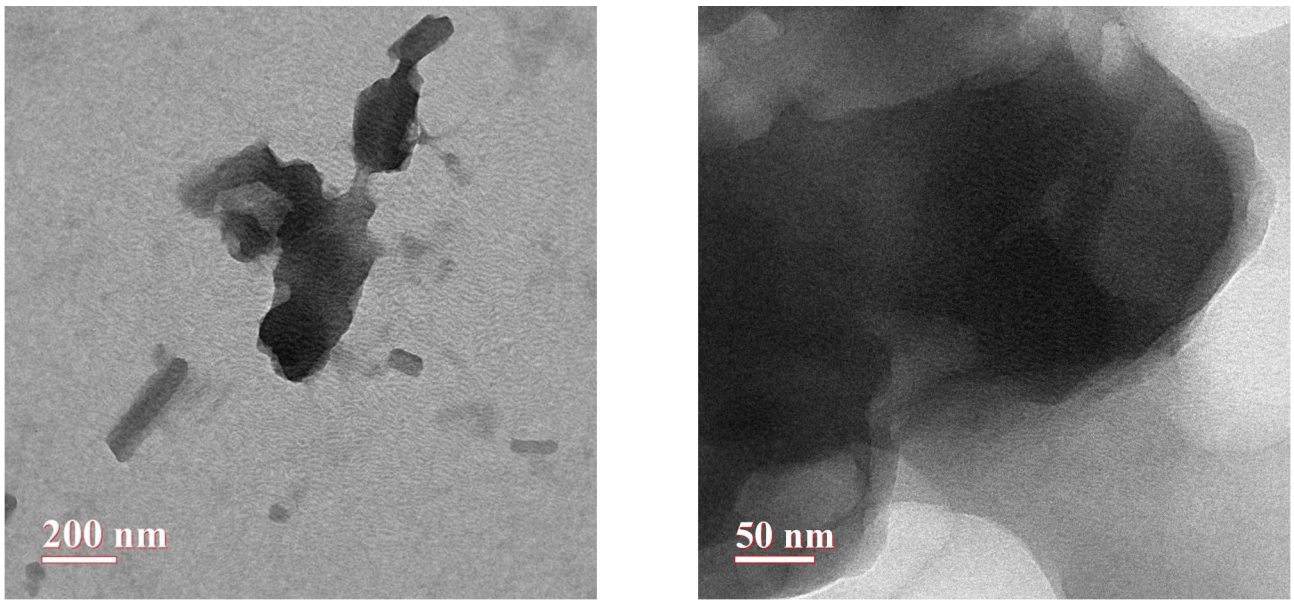

Fig. 6. TEM analysis of KPP catalyst.

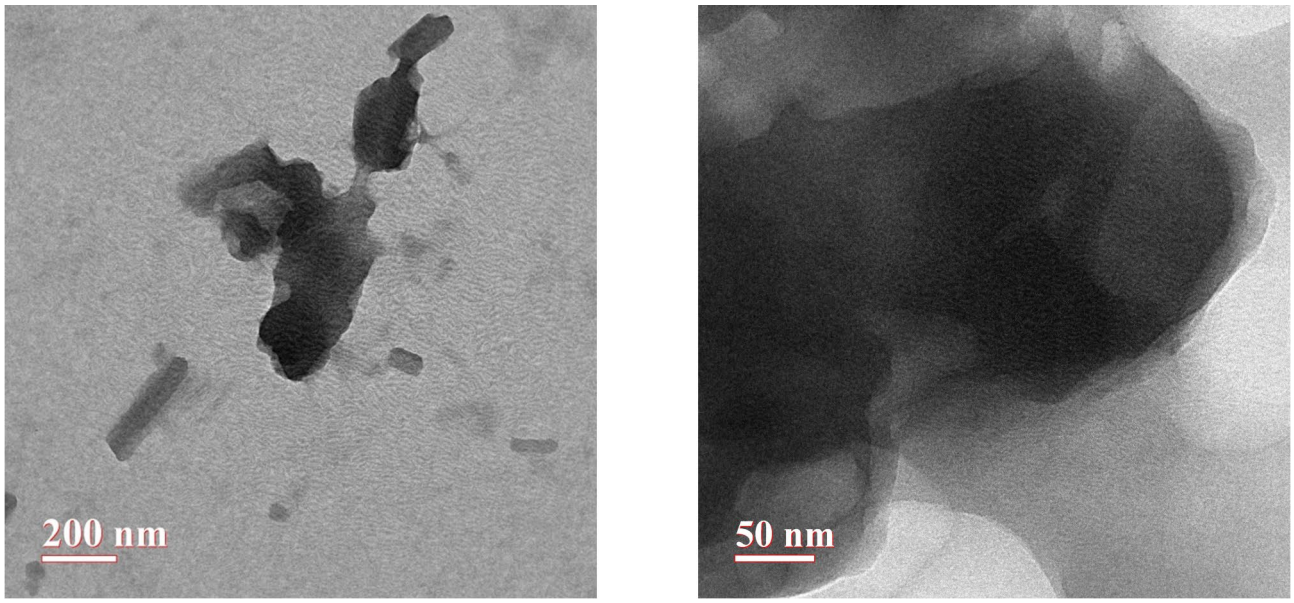

Fig. 7. SEM images of the KPP catalyst.

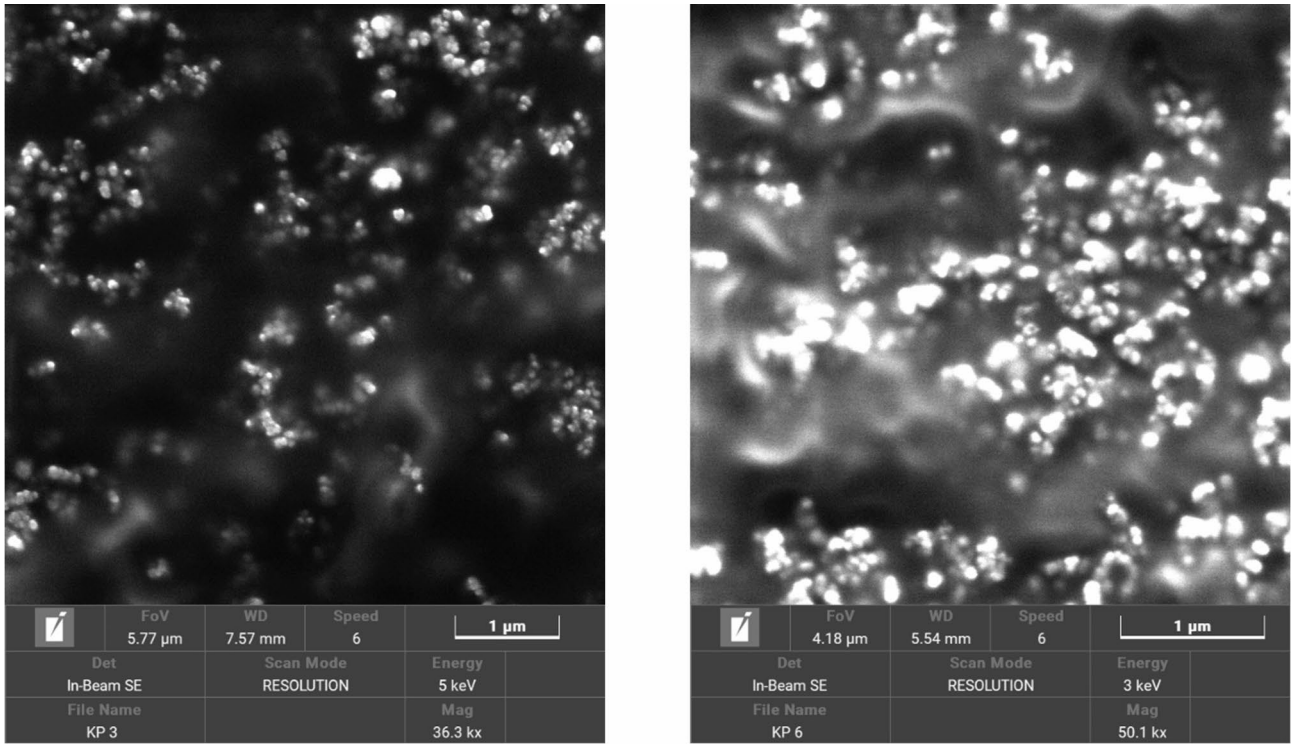

Fig. 8. SEM images of the recovered KPP catalyst after catalytic reaction.

As shown in Fig. 12, different peaks of fragmentations for the catalytic product of aniline and derivatives with epichlorohydrin are represented. The GC-MS spectra of catalytic product **3a** is represented in Fig. 12a, while Fig. 12b-d represented the catalytic products **3b-d** respectively.

We have also compared the catalytic activity of KPP with the previously reported sustainable catalyst for the synthesis of β-amino alcohol by ring opening of epoxide with amines (Table 5). The comparative study table reveals that our catalyst has high sustainability for the ring opening of the epoxide reaction.

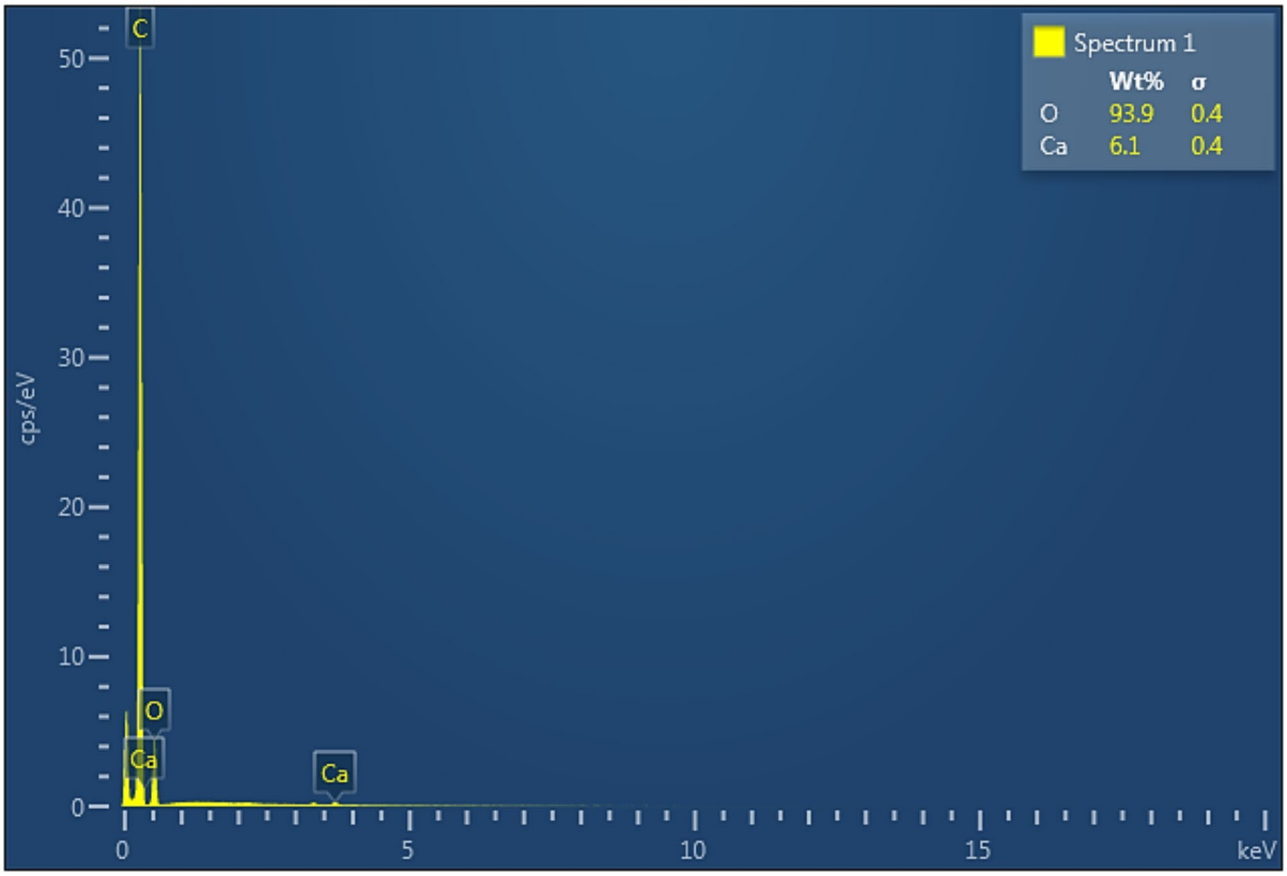

Fig. 9. EDX spectrum of KPP catalyst.

Recycling performance of KPP

The recycling of KPP was also performed for ring opening reaction of epichlorohydrin with aniline (Fig. 13) up to 5 cycles as shown in Table 6. It is observed that in the first two cycles, there is no loss in yield of catalytic product but in 3rd cycle, a 48% yield of 1-chloro-2-(phenylamino)ethan-1-ol is found. In the 4th and 5th cycles, 43% yield was found of relative product. We have also characterized the recycled catalyst by FTIR and SEM, demonstrating that the surface of the KPP changed after the catalytic reaction. Hence, KPP's catalytic activity decreases with the catalytic cycle's increase.

Conclusion

Kinnow peel powder developed as the green catalyst for the synthesis of 1-chloro-2-(phenylamino)ethan-1-ol and their derivatives by the reaction of ring opening of epichlorohydrin with amine and its derivatives. Moreover, the KPP recovered and reused for up to five cycles without suffering a sizable loss in β-amino alcohol production. Additionally, comparisons of the three derivatives' yields have been made. Through statistical analysis, it is found that the optimum combinations of three parameters that is the type of catalyst, catalyst loading, and amine derivatives give the maximum reaction yield when the type of catalyst is K-peel, the amount of catalyst is 30 mg, and the type of derivative is 4-MA, respectively.

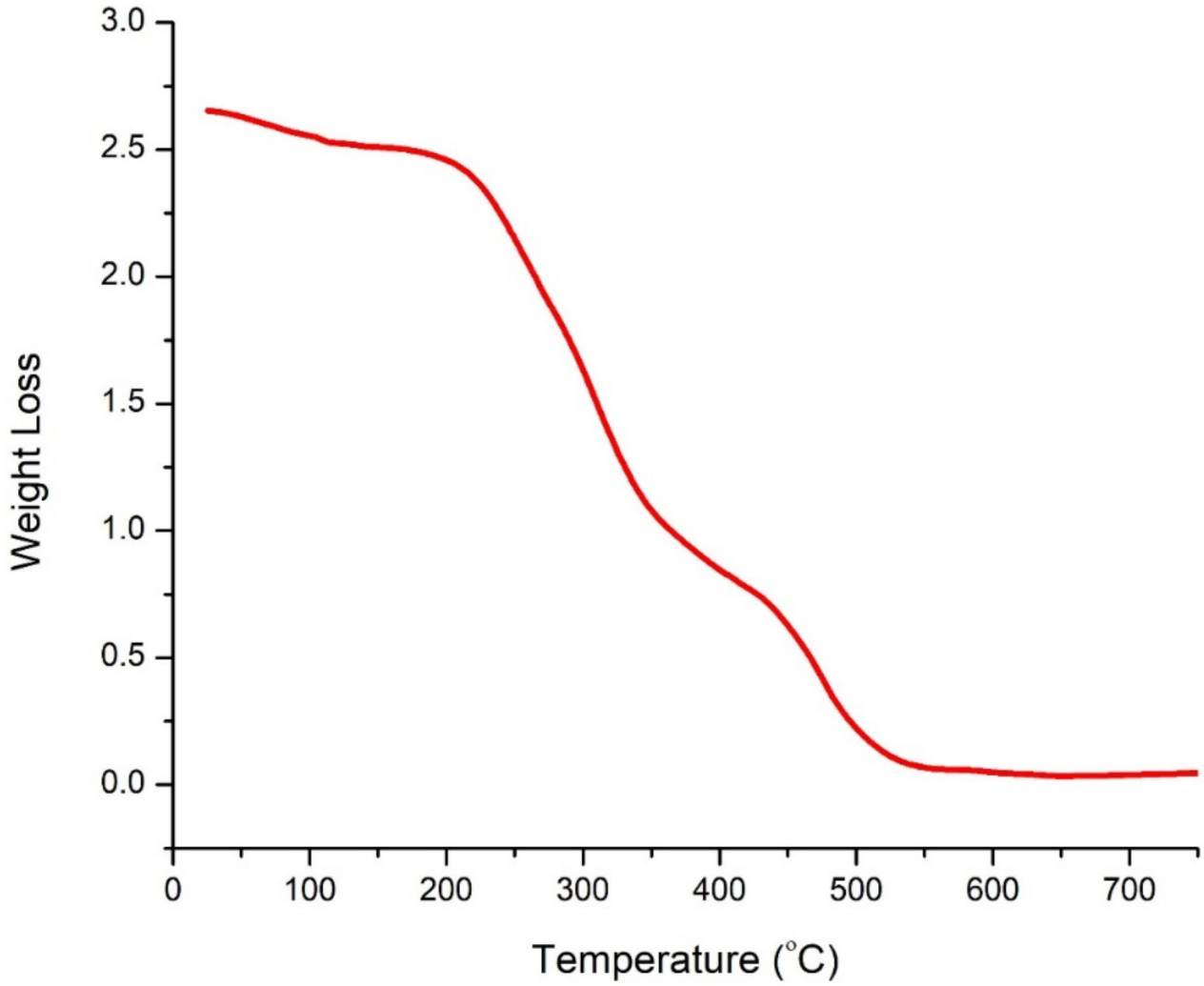

Fig. 10. TGA graph of KPP catalyst.

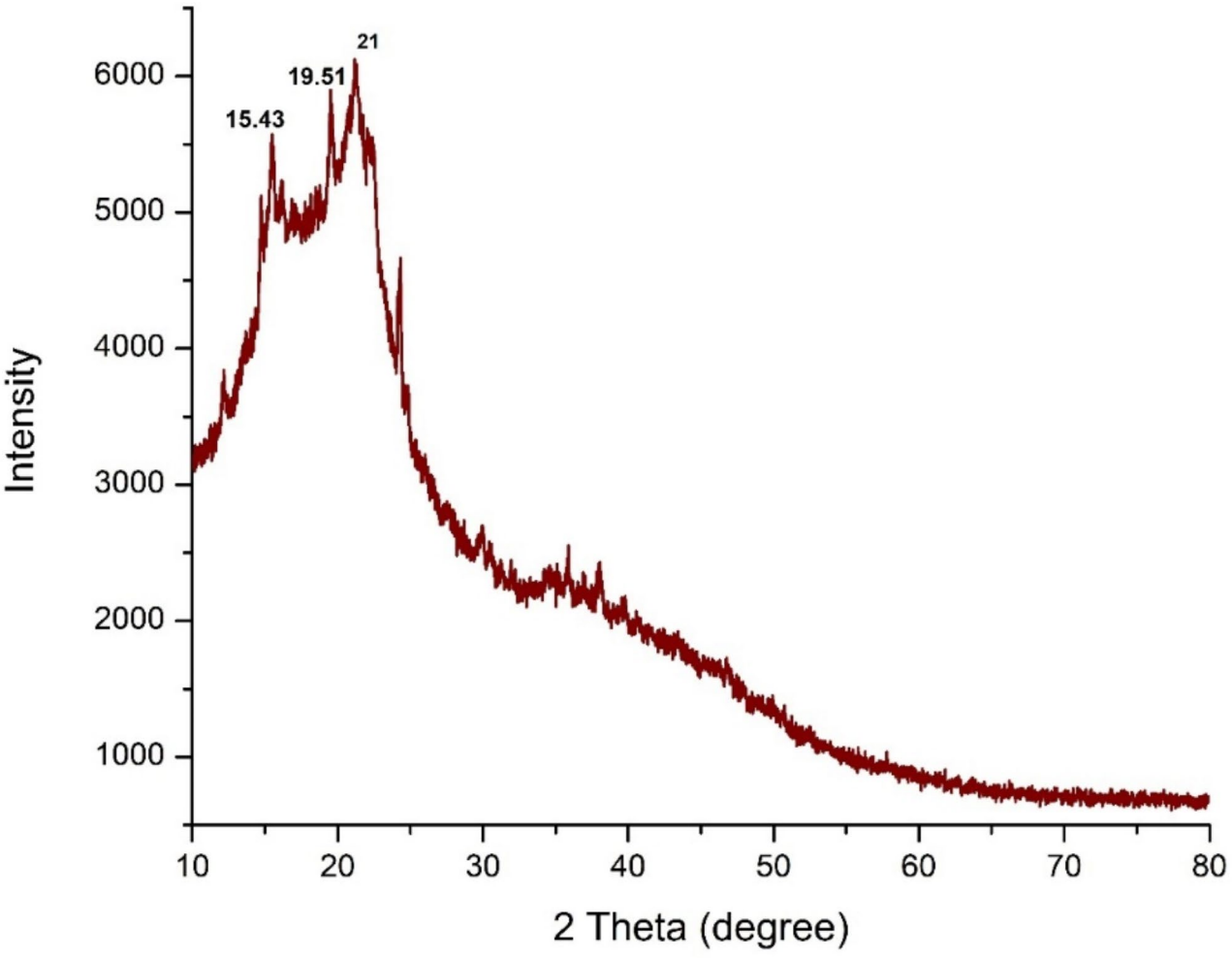

Fig. 11. XRD data of KPP catalyst.

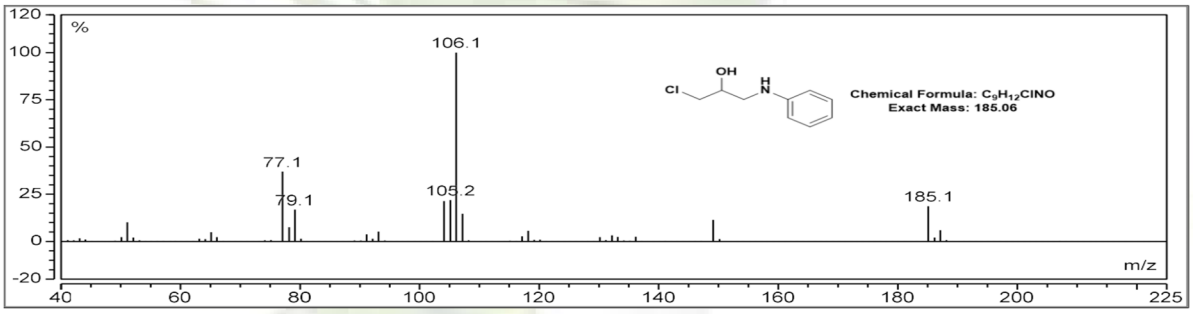

(a)

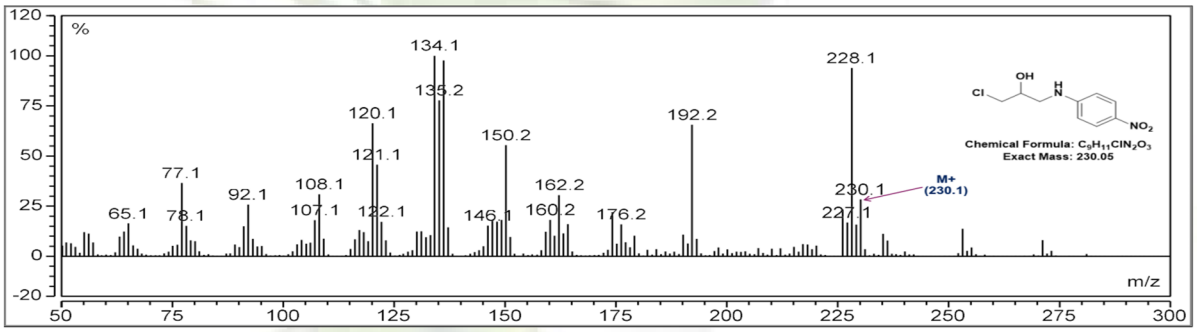

(b)

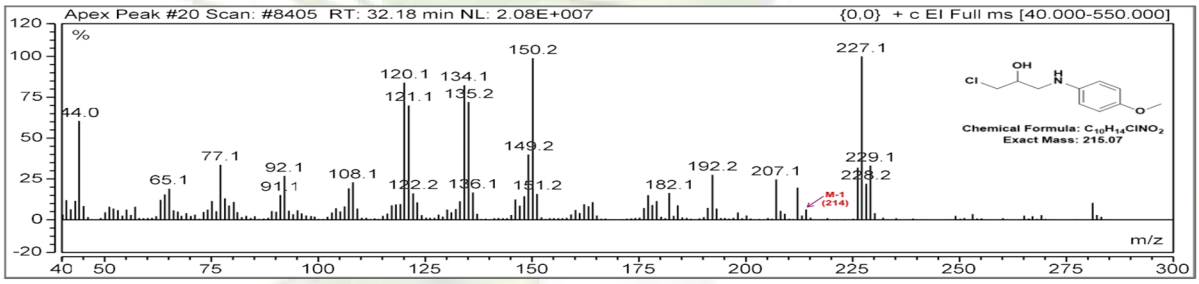

(c)

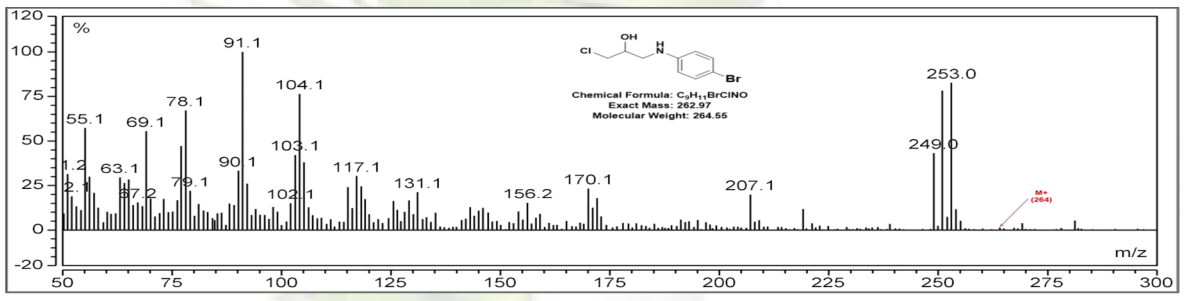

(d)

Fig. 12. GC-MS spectra of product 3a-d.

Catalyst	Reaction condition	Sustainability	%Yield of β amino alcohol	Refs.
1 M HCl in ether	0.5 mol % 1 M HCl in ether, toluene, rt, 3 h.	Metal free catalyst used	96–91	76
[Fe(BTC)]	epoxy (2.8 mmol), aniline (2.8 mmol), acetonitrile (4 mL), [Fe (BTC)] (50 mg), 40 °C, 16 h.	Recyclable Heterogenous catalyst	93–49	2
MCM type silica materials	MCM type mesoporous silica materials, epoxide (10 mmol), nucleophile (10 mmol), 6 h at 80 °C	Recyclable Heterogenous catalyst	99–43	77
$Bi(PO_4)$	$Bi(PO_4)$ (10 mol%), epoxide (1.0 mmol), amine (1.0 mmol), microwave irradiation (900 W)	microwave irradiation	88–24	78
IONs(0.00249 mmol of Fe, 2.493 10–4 mol% of Fe)	RT, Neat, 5 h	Recyclable catalyst	90	79
Mesoporous Zr-Beta	Epoxide (5 mmol), amine (5 mmol), 25 mg catalyst, 308 K, 0.5 h	Mesoporous recyclable catalyst	80	80
CoFe@rGO	epoxide (1 mmol), Amine (1 mmol), Catalyst 20%, 12 h, 80 °C	Magnetic recyclable catalyst	87	81
nano Fe_3O_4	RT, Neat, 20 h	Magnetic and neat condition	83	82
mesoporous TiO_2 -Fe_2O_3	Epoxide (1 mmol), amine (1 mmol), catalyst (20 mg), neat, 3 h, RT	Recyclable Porous nanomaterials	96	83
KPP	Epoxide (1 mmol), Amine (1 mmol), catalyst 30 mg, neat, 24 h, RT	Metal Free and fruit waste as recyclable catalyst	53	This work

Table 5. Comparative study table for the synthesis methods of β-amino alcohols using various catalysts.

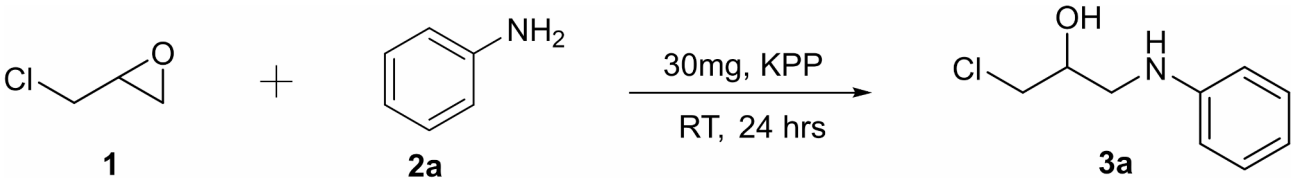

Fig. 13. Recycling performance of KPP for Ring opening of epichlorohydrin with aniline.

Entry	Cycle	%Yield
1	0	52
2	1	52
3	2	48
4	3	43
5	4	43

Table 6. Recycling performance of KPP for ring opening of epichlorohydrin with aniline.

Data availability

Data will be available on request and will be provided by the corresponding author.

Received: 28 June 2024; Accepted: 25 March 2025
Published online: 17 May 2025

References

1. Lin, S., Horsman, G. P. & Shen, B. Characterization of the epoxide hydrolase NcsF2 from the neocarzinostatin biosynthetic gene cluster. *Org. Lett.* **12** (17), 3816–3819 (2010).
2. Dhakshinamoorthy, A., Alvaro, M. & Garcia, H. Metal–organic frameworks as efficient heterogeneous catalysts for the regioselective ring opening of epoxides. *Chemistry–A Eur. J.* **16** (28), 8530–8536 (2010).
3. Das, S. & Asefa, T. Epoxide ring-opening reactions with mesoporous silica-supported Fe (III) catalysts. *ACS Catal.* **1** (5), 502–510 (2011).
4. Mohebbi, M., Salehi, P., Bararjanian, M. & Ebrahimi, S. N. Noscapine-derived β-amino alcohols as new organocatalysts for enantioselective addition of diethylzinc to aldehydes. *J. Iran. Chem. Soc.* **15** (1), 47–53 (2018).
5. Castejón, P., Moyano, A., Pericàs, M. A. & Riera, A. Ready access to stereodefined β-hydroxy-γ-amino acids. Enantioselective synthesis of fully protected cyclohexylstatine. *Tetrahedron* **52** (20), 7063–7086 (1996).
6. Alonso, D. A., Guijarro, D., Pinho, P., Temme, O. & Andersson, P. G. 3 R, 4 R)-2-Azanorbornylmethanol, an efficient ligand for Ruthenium-Catalyzed asymmetric transfer hydrogenation of ketones. *J. Org. Chem.* **63(8)** (1), 2749–2751 (1998).
7. Ager, D. J., Prakash, I. & Schaad, D. R. 1, 2-Amino alcohols and their heterocyclic derivatives as chiral auxiliaries in asymmetric synthesis. *Chem. Rev.* **96** (2), 835–876 (1996).
8. Nicolaou, K. C. & Boddy, C. N. Atropselective macrocyclization of diaryl ether ring systems: application to the synthesis of Vancomycin model systems. *J. Am. Chem. Soc.* **124** (35), 10451–10455 (2002).
9. Du, L. H. et al. Ring-Opening of epoxides with amines for synthesis of β-Amino alcohols in a Continuous-Flow biocatalysis system. *Catalysts* **10** (12), 1419 (2020).

10. Yamada, S. et al. A sustained increase in β-adrenoceptors during long-term therapy with Metoprolol and Bisoprolol in patients with heart failure from idiopathic dilated cardiomyopathy. *Life Sci.* **58** (20), 1737–1744 (1996).
11. Khirani, S. et al. Effect of salbutamol on respiratory muscle strength in spinal muscular atrophy. *Pediatr. Neurol.* **73**, 78–87 (2017).
12. Zhu, S., Meng, L., Zhang, Q. & Wei, L. Synthesis and evaluation of febrifugine analogues as potential antimalarial agents. *Bioorg. Med. Chem. Lett.* **16** (7), 1854–1858 (2006).
13. Ståhlberg, J. et al. Structural basis for enantiomer binding and separation of a common β-blocker: crystal structure of cellobiohydrolase Cel7A with bound (S)-propranolol at 1.9 Å resolution. *J. Mol. Biol.* **305** (1), 79–93 (2001).
14. Kumar, R. et al. Synthesis, crystal structure investigation, DFT analyses and antimicrobial studies of silver (I) complexes with N, N, N′, N′′-tetrakis (2-hydroxyethyl/propyl) Ethylenediamine and Tris (2-hydroxyethyl) amine. *New J. Chem.* **38** (3), 1186–1198 (2014).
15. Dohnálek, J. et al. Hydroxyethylamine isostere of an HIV-1 protease inhibitor prefers its amine to the hydroxy group in binding to catalytic aspartates. A synchrotron study of HIV-1 protease in complex with a peptidomimetic inhibitor. *J. Med. Chem.* **45** (7), 1432–1438 (2002).
16. Schmidt, B., Braun, H. A. & Narlawar, R. Drug development and PET-diagnostics for Alzheimer's disease. *Curr. Med. Chem.* **12** (14), 1677–1695 (2005).
17. Erdogan Orhan, I. & Sezer Senol, F. Designing multi-targeted therapeutics for the treatment of Alzheimer's disease. *Curr. Top. Med. Chem.* **16** (17), 1889–1896 (2016).
18. Tayade, K. N. et al. Zirconium triflate grafted on SBA-15 as a highly efficient solid acid catalyst for ring opening of epoxides by amines and alcohols. *Chin. J. Catal.* **38** (4), 758–766 (2017).
19. Natongchai, W., Khan, R. A., Alsalme, A. & Shaikh, R. R. YCl3-catalyzed highly selective ring opening of epoxides by amines at room temperature and under solvent-free conditions. *Catalysts* **7** (11), 340 (2017).
20. Prathap, K. J., Wu, Q., Olsson, R. T. & Dinér, P. Catalytic reductions and tandem reactions of nitro compounds using in situ prepared nickel boride catalyst in nanocellulose solution. *Org. Lett.* **19** (18), 4746–4749 (2017).
21. Karimi, M., Hajiashrafi, T., Heydari, A. & Azhdari Tehrani, A. Terbium–organic framework as heterogeneous Lewis acid catalyst for β-aminoalcohol synthesis: efficient, reusable and green catalytic method. *Appl. Organomet. Chem.*, **31**(12), e3866. (2017).
22. Tan, N. et al. Synthesis and structure of an air-stable organobismuth triflate complex and its use as a high-efficiency catalyst for the ring opening of epoxides in aqueous media with aromatic amines. *J. Organomet. Chem.* **696** (8), 1579–1583 (2011).
23. Ollevier, T. & Lavie-Compin, G. An efficient method for the ring opening of epoxides with aromatic amines catalyzed by bismuth trichloride. *Tetrahedron Lett.* **43** (44), 7891–7893 (2002).
24. Venkat Narsaiah, A., Reddy, B. V. S., Premalatha, K., Reddy, S. S. & Yadav, J. S. Bismuth (III)-catalyzed hydrolysis of epoxides and aziridines: an efficient synthesis of vic-diols and β-amino alcohols. *Catal. Lett.* **131**, 480–484 (2009).
25. Bansal, S. et al. An efficient method for regioselective ring opening of epoxides by amines under microwave irradiation using Bi (3) 3· 5H 2 O as a catalyst. *New J. Chem.* **41** (7), 2668–2671 (2017).
26. Kayan, A. Synthesis of Poly (styrene oxide) with different molecular weights using Tin catalysts. *Des. Monomers Polym.* **18** (6), 545–549 (2015).
27. Kayan, A. Copolymerization reactions of butadiene monoxide with 3-glycidyloxypropyltrimethoxysilane and styrene oxide and their glycol derivatives. *J. Appl. Polym. Sci.* **136** (14), 47074 (2019).
28. Kayan, A. Polymerization of 3-glycidyloxypropyltrimethoxysilane with different catalysts. *J. Appl. Polym. Sci.* **123** (6), 3527–3534 (2012).
29. Mason, T. J. & Sonochemistry Oxford University Press: Oxford, (1999).
30. Chalmers, J. M. *Spectroscopy in Process Analysis* (CRC, 2000).
31. Bargon, J. & Kuhn, L. T. (eds) *Situ NMR Methods in Catalysis* (Springer, 2007).
32. Bose, A. K., Manhas, M. S., Ganguly, S. N., Sharma, A. H. & Banik, B. K. More chemistry for less pollution: applications for process development. *Synthesis* **2002** (11), 1578–1591 (2002).
33. Nüchter, M., Ondruschka, B., Bonrath, W. & Gum, A. Microwave assisted synthesis–a critical technology overview. *Green Chem.* **6** (3), 128–141 (2004).
34. Larhed, M. & Olofsson, K. (eds) *Microwave Methods in Organic Synthesis*Vol. 266 (Springer, 2006).
35. Anastas, P. T. & Warner, J. C. *Green Chemistry: Theory and Practice* (Oxford University Press: Oxford, U.K.,, 1998).
36. Grison, C. & Ki, Y. L. T. Ecocatalysis, a new vision of green and sustainable chemistry. *Curr. Opin. Green. Sustainable Chem.* **29**, 100461 (2021).
37. Deyris, P. A. & Grison, C. Nature, ecology and chemistry: an unusual combination for a new green catalysis, ecocatalysis. *Curr. Opin. Green. Sustainable Chem.* **10**, 6–10 (2018).
38. Grison, C., Escande, V. & Olszewski, T. K. Ecocatalysis: a new approach toward bioeconomy. In Bioremediation and Bioeconomy (629–663). Elsevier. (2016).
39. Zhu, B., Qiu, K., Shang, C. & Guo, Z. Naturally derived porous carbon with selective metal-and/or nitrogen-doping for efficient CO 2 capture and oxygen reduction. *J. Mater. Chem. A*. **3** (9), 5212–5222 (2015).
40. Sevilla, M., Ferrero, G. A. & Fuertes, A. B. One-pot synthesis of biomass-based hierarchical porous carbons with a large porosity development. *Chem. Mater.* **29** (16), 6900–6907 (2017).
41. Veerakumar, P. et al. Porous carbon-modified electrodes as highly selective and sensitive sensors for detection of dopamine. *Analyst* **139** (19), 4994–5000 (2014).
42. Madhu, R., Karuppiah, C., Chen, S. M., Veerakumar, P. & Liu, S. B. Electrochemical detection of 4-nitrophenol based on biomass derived activated carbons. *Anal. Methods*. **6** (14), 5274–5280 (2014).
43. Veeramani, V. et al. Heteroatom-enriched porous carbon/nickel oxide nanocomposites as enzyme-free highly sensitive sensors for detection of glucose. *Sens. Actuators B*. **221**, 1384–1390 (2015).
44. Veeramani, V. et al. Cajeput tree bark derived activated carbon for the practical electrochemical detection of Vanillin. *New J. Chem.* **39** (12), 9109–9115 (2015).
45. Liu, L., Zhu, Y. P., Su, M. & Yuan, Z. Y. Metal-free carbonaceous materials as promising heterogeneous catalysts. *ChemCatChem* **7** (18), 2765–2787 (2015).
46. Subodh, Mogha, N. K., Chaudhary, K., Kumar, G. & Masram, D. T. Fur-imine-functionalized graphene oxide-immobilized copper oxide nanoparticle catalyst for the synthesis of Xanthene derivatives. *ACS Omega*. **3** (11), 16377–16385 (2018).
47. Sun, X. et al. Single Cobalt sites in mesoporous N-doped carbon matrix for selective catalytic hydrogenation of nitroarenes. *J. Catal.* **357**, 20–28 (2018).
48. Veerakumar, P., Dhenadhayalan, N., Lin, K. C. & Liu, S. B. Highly stable ruthenium nanoparticles on 3D mesoporous carbon: an excellent opportunity for reduction reactions. *J. Mater. Chem. A*. **3** (46), 23448–23457 (2015).
49. Veerakumar, P. et al. Biomass-derived activated carbon supported Fe3O4 nanoparticles as recyclable catalysts for reduction of nitroarenes. *ACS Sustain. Chem. Eng.* **4** (12), 6772–6782 (2016).
50. Balahmar, N., Al-Jumialy, A. S. & Mokaya, R. Biomass to porous carbon in one step: directly activated biomass for high performance CO 2 storage. *J. Mater. Chem. A*. **5** (24), 12330–12339 (2017).
51. Manyà, J. J., González, B., Azuara, M. & Arner, G. Ultra-microporous adsorbents prepared from vine shoots-derived Biochar with high CO2 uptake and CO2/N2 selectivity. *Chem. Eng. J.* **345**, 631–639 (2018).
52. Zhang, C. et al. Porous carbons derived from hypercrosslinked porous polymers for gas adsorption and energy storage. *Carbon* **114**, 608–618 (2017).

53. Chang, H., Joo, S. H. & Pak, C. Synthesis and characterization of mesoporous carbon for fuel cell applications. *J. Mater. Chem.* **17** (30), 3078–3088 (2007).
54. Jain, A. et al. Highly mesoporous carbon from Teak wood sawdust as prospective electrode for the construction of high energy Li-ion capacitors. *Electrochim. Acta*. **228**, 131–138 (2017).
55. Ma, H., Liu, Z., Wang, X., Zhang, C. & Jiang, R. Supercapacitive performance of porous carbon materials derived from tree leaves. *J. Renew. Sustain. Energy*, **9**(4). (2017).
56. Tang, W. et al. Natural biomass-derived carbons for electrochemical energy storage. *Mater. Res. Bull.* **88**, 234–241 (2017).
57. Wang, J. et al. Biomass derived carbon for energy storage devices. *J. Mater. Chem. A*. **5** (6), 2411–2428 (2017).
58. Zhang, G., Chen, Y., Chen, Y. & Guo, H. Activated biomass carbon made from bamboo as electrode material for supercapacitors. *Mater. Res. Bull.* **102**, 391–398 (2018).
59. Yao, Y. et al. Synthesis of sea urchin-like carbon nanotubes/porous carbon superstructures derived from waste biomass for treatment of various contaminants. *Appl. Catal. B*. **219**, 563–571 (2017).
60. Zhu, L. et al. An environmentally friendly carbon aerogels derived from waste pomelo peels for the removal of organic pollutants/oils. *Microporous Mesoporous Mater.* **241**, 285–292 (2017).
61. Verma, R. et al. Synthesis of N-Benzylideneaniline by schiff base reaction using Kinnow Peel powder as green catalyst and comparative study of derivatives through ANOVA techniques. *Sci. Rep.* **12** (1), 9636 (2022).
62. Ahirrao, D. J., Tambat, S., Pandit, A. B. & Jha, N. Sweet-Lime-Peels-Derived Activated-Carbon-Based electrode for highly efficient supercapacitor and Flow-Through water desalination. *ChemistrySelect* **4** (9), 2610–2625 (2019).
63. Senophiyah-Mary, J., Thomas, T., Loganath, R. & Meenambal, T. Optimisation of Copper Removal from E-Waste Using Bioleaching Technique by Activated Mosambi Peels. In *Waste Valorisation and Recycling: 7th IconSWM—ISWMAW 2017, Volume 2* (pp. 363–371). Springer Singapore. (2019).
64. Yadav, S. & Sharma, C. S. Novel and green processes for citrus Peel extract: a natural solvent to source of carbon. *Polym. Bull.* **75**, 5133–5142 (2018).
65. Bhatnagar, A., Sillanpää, M. & Witek-Krowiak, A. Agricultural waste peels as versatile biomass for water purification–A review. *Chem. Eng. J.* **270**, 244–271 (2015).
66. Mondal, N. K., Basu, S., Sen, K. & Debnath, P. Potentiality of Mosambi (Citrus limetta) Peel dust toward removal of cr (VI) from aqueous solution: an optimization study. *Appl. Water Sci.* **9**, 1–13 (2019).
67. Grison, C., Escande, V. & Biton, J. *Ecocatalysis: A New Integrated Approach To Scientific Ecology* (Elsevier, 2015).
68. Grison, C. Combining phytoextraction and ecocatalysis: a novel concept for greener chemistry, an opportunity for remediation. *Environ. Sci. Pollut. Res.* **22**, 5589–5591 (2015).
69. Osman, A. I. et al. Coordination-driven innovations in low-energy catalytic processes: advancing sustainability in chemical production. *Coord. Chem. Rev.* **514**, 215900 (2024).
70. Osman, A. I., Zhang, Y., Farghali, M., Rashwan, A. K., Eltaweil, A. S., Abd El-Monaem,E. M., … Yap, P. S. (2024). Synthesis of green nanoparticles for energy, biomedical,environmental, agricultural, and food applications: A review. Environmental Chemistry Letters, 22(2), 841–887.
71. Osman, A. I. Mass spectrometry study of lignocellulosic biomass combustion and pyrolysis with nox removal. *Renew. Energy*. **146**, 484–496 (2020).
72. Zapata, B., Balmaseda, J., Fregoso-Israel, E. & Torres-García, E. Thermo-kinetics study of orange Peel in air. *J. Therm. Anal. Calorim.* **98** (1), 309–315 (2009).
73. Akinhanmi, T. F. et al. Orange Peel as low-cost adsorbent in the elimination of Cd(II) ion: kinetics, isotherm, thermodynamic and optimization evaluations. *Bioresour Bioprocess.* **7**, 34 (2020).
74. Das, A., Anbu, N., Reinsch, H., Dhakshinamoorthy, A. & Biswas, S. A thiophene-2-carboxamide-functionalized Zr (IV) organic framework as a prolific and recyclable heterogeneous catalyst for regioselective ring opening of epoxides. *Inorg. Chem.* **58** (24), 16581–16591 (2019).
75. Nakhate, A. V., Doke, S. M. & Yadav, G. D. Template assisted synthesis of nanocrystalline sulfated Titania: active and robust catalyst for regioselective ring opening of epoxide with aniline and kinetic modeling. *Ind. Eng. Chem. Res.* **55** (41), 10829–10838 (2016).
76. Tyagi, A., Yadav, N., Khan, J., Mondal, S. & Hazra, C. K. Brønsted Acid-Catalysed epoxide Ring-Opening using amine nucleophiles: A facile access to β-Amino alcohols. *Chemistry–An Asian J.*, **17**(14), e202200379. (2022).
77. Pandey, M., Tsunoji, N., Kubota, Y. & Bandyopadhyay, M. Amine and sulfonic acid anchored porous silica as recyclable heterogeneous catalysts for Ring-Opening of oxiranes. *ChemistrySelect*, **7**(30), e202201756. (2022).
78. Gupta, D. & Singh, P. P. Environment benign bismuth based catalysts for the expedite regioselective ring opening of epoxides under solvent free microwave condition. *ChemistrySelect*, **9**(15), e202303373. (2024).
79. Halder, M., Roy, A. S. & Sen, K. Aromatic amine mediated ring opening of epoxides: A reaction catalyzed by biogenic iron oxide nanoparticles. *J. Indian Chem. Soc.* **98** (6), 100056 (2021).
80. Tang, B. et al. Mesoporous Zr-Beta zeolites prepared by a post-synthetic strategy as a robust Lewis acid catalyst for the ring-opening aminolysis of epoxides. *Green Chem.* **17** (3), 1744–1755 (2015).
81. Sheoran, A., Kaur, J., Kaur, P., Kumar, V., Tikoo, K. B., Agarwal, J., … Singhal,S. (2020). Graphene based magnetic nanohybrids as promising catalysts for the green synthesis of β-amino alcohol derivatives. Journal of Molecular Structure, 1204, 127522.
82. Kumar, A., Parella, R. & Babu, S. A. Magnetic nano Fe3O4 catalyzed solvent-free stereo-and regioselective aminolysis of epoxides by amines; A green method for the synthesis of β-amino alcohols. *Synlett* **25** (06), 835–842 (2014).
83. Roy, S., Banerjee, B., Salam, N., Bhaumik, A. & Islam, S. M. Mesoporous titania-iron (III) oxide with nanoscale porosity and high catalytic activity for the synthesis of β-amino alcohols and benzimidazole derivatives. *ChemCatChem* **7** (17), 2689–2697 (2015).

Acknowledgements

We express our sincere gratitude to Amity University, Jaipur, Rajasthan, for lending us their laboratory space. The authors express their gratitude to the Rajasthan State Pollution Control Board for the grant F12/(Project-282) RSPCB/Project/3491-3495 and DST-PURSE program, Govt. of India (SR/PURSE/2021/77) for the financial support provided to the Chemistry Department at the Amity School of Applied Sciences, Amity University Rajasthan, Jaipur.

Author contributions

RT has conducted experiments, NPL has edited the manuscript, JP has done the statistical study, SCS has monitored the experiments and MSC has designed the experiments. PB has contributed in the GC-MS characterization of the product, VB has contributed to the technical discussion of data interpretation of GC-MS data. and UKS has contributed to SEM and TEM characterization of KPP.

Declarations

Competing interests
The authors declare no competing interests.

Additional information
Correspondence and requests for materials should be addressed to S.C.S. or M.S.C.

Reprints and permissions information is available at www.nature.com/reprints.

Publisher's note Springer Nature remains neutral with regard to jurisdictional claims in published maps and institutional affiliations.